


Influence of milk fat on the physicochemical property of nanoencapsulated curcumin and enhancement of its biological properties thereof

Pooja J. Rao¹  · Hafeeza Khanum¹ ·
Pushpa S. Murthy¹ · S. V. Shreelakshmi² ·
Maria Sheeba Nazareth²

Revised: 5 December 2022 / Accepted: 29 January 2023 / Published online: 12 February 2023
© Association of Food Scientists & Technologists (India) 2023

Abstract Curcumin, bioactive from turmeric *Curcuma longa*, has been known for its therapeutic properties. However, its lipophilic nature and poor bioavailability are the constraints to harnessing its properties. Encapsulation in nano-size helps to alleviate the constraints and enhance its biological properties due to its higher surface area. The study aims to encapsulate curcumin in a nanometer size range by solubilizing in lipid (milk fat) and using milk protein as a water-soluble carrier. The lipid:curcumin ratio (1:0.05, 1:0.1, 1:0.2, 1.5:0.1, 1.5:0.2, 2.0:0.1 and 2:0.2% (w/w)) produced nanoemulsion with droplets sizes 30–200 nm. The sample containing lipid: curcumin, as 1.0:0.05 resulted in an encapsulation efficiency of 92.6%, and its binding interaction with the carrier, was $K_D = 4.7 \mu\text{M}$. A high solubility of curcumin in milk fat and digestion during in vitro lipolysis increased its bioaccessibility. A simulated gastro-intestinal in vitro studies showed that cumulative release percentage of nanoencapsulated curcumin was 60% at pH 7.4 compared to 0.8% of native curcumin. The anti-microbial property of nanoencapsulated curcumin was more potent than native curcumin against food pathogenic organisms such as *S. aureus*, *B. cereus*, *E. coli*, *B. subtilis*, *P. aeruginosa*, *P. aeruginosa*, *C. violaceum*.

Keywords Nanoencapsulation · Milk-fat solubilized curcumin · Binding interaction · *In-vitro* bioaccessibility · Anti-microbial activity

Abbreviations

Biological, Chemical and Microbiological

GRAS	Generally regarded as safe
SCT	Short-chain triglycerides
MCT	Medium-chain triglycerides
LCT	Long-chain triglycerides
NCP	Nanoencapsulated curcumin powder
NaCas	Sodium caseinate
BCA	Bicinchoninic acid
EE	Encapsulation efficiency
g	Gram
PBS	Phosphate-buffered saline
ABTS	2,2'-Azino-bis(3-ethylbenzothiazoline-6-sulphonic acid)
CFU	Colony forming units

Instrumental techniques

SEM	Scanning electron microscopy
FTIR	Fourier transform infrared
MST	Microscale thermophoresis
UV	Ultra violet
Vis	Visible

Supplementary Information The online version contains supplementary material available at <https://doi.org/10.1007/s13197-023-05684-5>.

✉ Pooja J. Rao
poojarao@cftri.res.in

¹ Plant Products, Spices and Flavour Sciences Department, Council of Scientific and Industrial Research–Central Food Technological Research Institute, Mysuru 570020, India

² Plant Cell Bio-Technology, Central Food Technological Research Institute, Mysuru 570020, India

Introduction

The synthesis and design of compounds and devices at nano-scale (< 100 nm) has led to a revolutionary change in the field of science and its applications. The influence of nano-science and nanotechnology in the food sector is gaining

momentum for the development of nutraceutical and functional foods. The bioactive compounds of plants, possessing significant therapeutic properties, can be processed using different techniques to restrict their growth at the nano-scale and to incorporate them into different food products. Curcumin, a bioactive compound from the spice turmeric (*Curcuma longa*), possesses several biological properties such as anti-microbial (Paula et al. 2018), anti-oxidant (Deck et al. 2018), anti-cancerous, anti-inflammatory (Sun et al. 2013), and anti-viral properties. Thus, it can be used for enhancing the shelf life of food products and the prevention/treatment of diseases. However, its lipophilic nature with low bioavailability is a limiting factor to harness the aforementioned properties. The enhancement of its water solubility has been reported (Shankar Patel et al. 2022) (Pandey et al. 2022) by arresting the particle growth at nano-scale (50–500 nm), using different water-soluble carrier materials, and employing high-energy techniques. The use of chemical solvents such as dichloromethane, ethanol, methanol, etc. (Bhawana et al. 2011) and carrier materials that do not have 'generally regarded as safe' (GRAS) status in curcumin nanoparticle synthesis, limit the use of nanoencapsulated curcumin in the food industry. There are reports mentioning protein, lipid, polysaccharides, biodegradable polymer, and carbohydrates as carrier materials (Bucurescu et al. 2018) (Peng et al. 2020) (Sheikhzadeh et al. 2016). However, the particle size was in the range of 150–350 nm with an encapsulation efficiency of 80–95%, and the raw materials and synthesis processes were not cost-effective.

The enhanced bioavailability of bioactive compounds is significantly influenced by the size of the nanoparticle, release kinetics of core (bioactive), and its interaction with carrier and lipid solubilizer. The solubilization percent of curcumin in lipid is important to estimate the amount available for gastrointestinal digestion during the lipolytic process (Ahmed et al. 2012). The solubility of curcumin in MCT-60, palm oil, butter, and olive oil, have been reported as 0.40, 0.35, 0.30, 0.2, mg mL⁻¹, respectively, and 2.98% in tributyrin (short-chain triglyceride) (Jiang and Charcosset 2022) (Kumar et al. 2016). However, it is interesting to quantify the solubility of curcumin in the milk fat that contains short-chain triglycerides (SCT)/medium-chain triglycerides (MCT)/long-chain triglycerides (LCT) in different proportions wherein short-chain triglycerides form 40% of the mixture (<http://www.agroscope.admin.ch/milchfett/index.html?lang=en>, 2015).

In our previous work (Rao and Khanum 2016), the nanoencapsulation of curcumin was reported by varying the amount of carrier, sodium caseinate, and its physicochemical characteristics were analyzed. In the present investigation, core material, and lipid-curcumin ratio, have been varied and their effect on the physical and chemical properties of nanoencapsulated curcumin powder (NCP) have been studied. The NCP with

high encapsulation efficiency was assessed for in vitro bioaccessibility, lipolytic action, anti-oxidant and anti-microbial properties. The selection of carrier material is an important aspect of encapsulation due to its binding affinity with the core. Sodium caseinate was preferred as wall material because of its purity, easy handling at room temperature, the small size of casein micelles in the range of 40–300 nm with an average size of 150 nm (Walstra et al. 2005), and mineral binding properties (Vegarud et al. 2000).

Materials and methods

The bioactive compound, Curcumin, used in the study was 95% pure and was procured from Salutaris Tech Pvt Ltd., Mysore, India. Milk fat (Nandini, Mysore, Karnataka, India) was used as a lipid and curcumin solubilizer. Sodium caseinate (NaCas) was purchased from Sigma-Aldrich, India. Tris maleate, sodium taurodioxycholate, and phosphatidylcholine were purchased from Sigma-Aldrich, and NaCl (GR), CaCl₂·2H₂O (GR) from Merck. Triple distilled (TD) water was used in all the preparations.

Preparation of nanoencapsulated curcumin

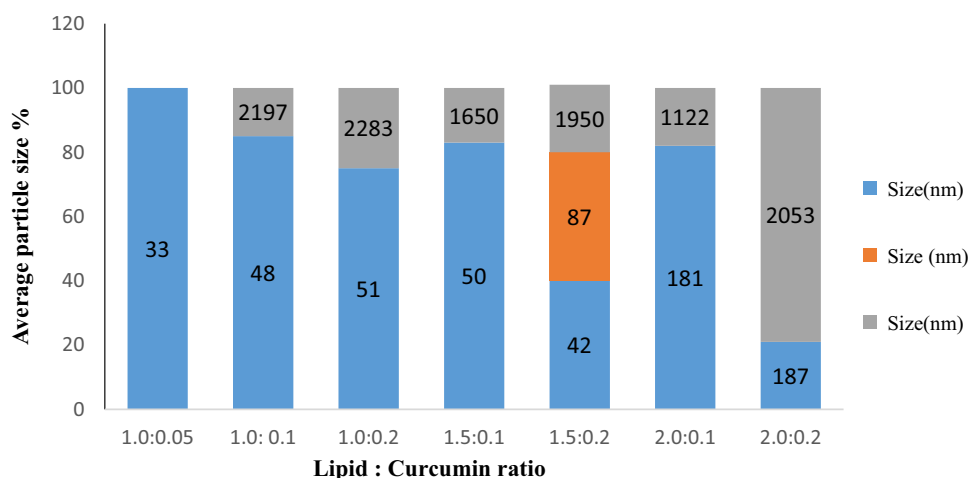
The nanoemulsion encapsulating curcumin was prepared by following the oil-in-water (o/w) method as mentioned earlier (Rao and Khanum 2016) with a slight modification. Milk fat was used as a curcumin solubilizer and the mixture was sonicated (Branson, Model-1510E) in a water bath at a temperature of 60 °C for 5–7 min. The milk fat:curcumin ratio was varied from 1:0.05, 1:0.1, 1:0.2, 1.5:0.1, 1.5:0.2, 2.0:0.1 and 2:0.2% (w/w) and the sodium caseinate (NaCas) amount was kept constant at 5% (by weight) for all the samples. The milk fat and curcumin were added to sodium caseinate solution and homogenized (IKA T25 digital ULTRA-TURRAX) at ~ 15,000 rpm speed followed by sonication (Sonics & Mat. Inc., Model-VC 750, Power 750 watts, Freq. 20 kHz) for 30 min to prepare nanoencapsulated curcumin (Fig. 1). The nanoemulsion was spray dried (SD, LSD-48, mini Spray Dryer, JISL) at inlet and outlet temperature of 110° and 60 °C, respectively to obtain NCP. All samples were prepared in triplicates and analyzed. The native sodium caseinate without lipid and core was also homogenized and ultrasonicated to be used as a control (treated sodium caseinate) for morphological and protein estimation.

Nanoparticle characterization

Morphology and particle size

As mentioned in the earlier research paper (Rao et al., 2016), the instrument Tri-LASER Diffraction Technology (TLDT; Model – Blue Wave, Microtrac, USA) was used

Fig. 1 Influence of lipid:curcumin ratio on the average particle size (%) of nanoemulsions



to analyze the distribution of particles in nanoemulsion and the spray-dried powder. The morphology of samples sprayed on aluminum sheets was examined using scanning electron microscopic (SEM; model/make: LEO435VP, Cambridge, UK) images. The particle size of dried powder was ascertained using transmission electron microscopy (TEM, Model: Tecnai G2 Spirit Bio-TWIN operating at 120 kV).

Fourier transform infrared (FTIR) spectroscopy

FTIR spectra of curcumin, native NaCas, and NCP were recorded using an FTIR spectrophotometer (Model: Platinum ATR, TENSOR II, Make: Bruker) and compared. A few milligrams of the powder samples were placed on the diamond crystal disk and the measurements were taken from 3500 to 500 cm^{-1} .

Protein and fat estimation

The amount of protein content in treated sodium caseinate and the nanoencapsulated samples was calculated using the bicinchoninic acid (BCA) kit method. The encapsulated fat was estimated as per the protocol (Fuchs et al. 2006) with slight modification. One gram sample was dissolved in hexane to remove surface-bound lipid and the solvent was evaporated on the rotary evaporator. The dry sample was dissolved in water and magnetically stirred for around 2 h. The

solution was transferred in a separating funnel, mixed with hexane, and allowed to stand for 45 min until a clear organic layer was formed. The organic fraction was collected and the process was repeated five times. The organic solvent from collected fractions was evaporated using a rotary evaporator (Heidolph, Germany) and the weight of the dry sample was calculated.

Encapsulation efficiency of nanoparticles

Encapsulation efficiency (EE) and loading concentration were determined as per the procedure reported (Rao and Khanum 2016). Briefly, 10 mg of NCP samples were dissolved in 5 ml of water and vortexed for 10 min. The solution was stored at room temperature (27 ± 1 °C) for 1 h and then centrifuged at 7000 g for 20 min. The free curcumin in the sample was determined by collecting the precipitates and by dissolving them in acetone. The acetone was used as a blank while recording UV absorbance at 420 nm. The amount of curcumin was calculated as given below (Surassmo et al. 2010)(Method 18, 1997);

$$\begin{aligned} \text{Actual curcumin in the yield NCP (g)} \\ = \text{Total amount of curcumin used (g)} \\ - \text{Free curcumin in the yield by UV measurement (g)} \end{aligned} \quad (1)$$

$$\text{Encapsulation Efficiency (\%)} = \left[\frac{\text{Actual curcumin in the yield (g)}}{\text{Total amount of curcumin (g)}} \right] \times 100 \quad (2)$$

$$\begin{aligned} \text{Theoretical Loading Concentration (\%)} \\ = \left[\frac{\text{Total amount of curcumin used (g)}}{\text{total mass of curcumin, lipid and sodium caseinate (g)}} \right] \times 100 \end{aligned} \quad (3)$$

$$\text{Actual Loading Concentration (\%)} = \left[\frac{\text{Actual curcumin in the yield (g)/ total mass of curcumin,}}{\text{lipid and sodium caseinate (g)}} \right] \times 100 \quad (4)$$

$$\text{Loading Efficiency (\%)} = \left[\frac{\text{Actual Loading Con.}}{\text{Theoretical Loading Con.}} \right] \times 100 \quad (5)$$

Binding affinity

The binding properties of protein-rich sodium caseinate with curcumin were investigated using the microscale thermophoresis (MST) (Monolith NT.115 MST instrument, NanoTemper Technologies GmbH, Munich Germany) technique (Seidel et al., 2013). The 40% of the blue LED (488 nm) and 1 V IR-laser power was used to excite the curcumin molecule which, has an autofluorescence. Laser on and off times was set at 35 s and 5 s, respectively. Standard treated capillaries from NanoTemper were used. Curcumin was dissolved in milk fat and bath-sonicated at 60 °C followed by centrifugation to collect the supernatant. Methanol was added to the curcumin-fat supernatant solution to collect the curcumin and fat was collected in hexane. The concentration of curcumin fluorescent molecule [A₀] was kept constant (40 nM) during the experiments and the concentration of ligand [L₀], sodium caseinate, varied in a dilution series (from 20 μM to 0.61 nM). The changes in fluorescence in a temperature gradient due to binding interaction was measured using the following equation:

$$F_{norm} = \frac{F_{hot}}{F_{cold}} \quad (6)$$

where F_{hot} is the fluorescence after thermodiffusion and F_{cold} is the initial fluorescence. By fitting F_{norm} as a function of the protein concentration K_D, the dissociation constant, was calculated using the following equation from the law of mass action,

$$K_D = \frac{[A] * [L]}{[AL]} \quad (7)$$

where [A] is the concentration of free curcumin molecule, [L] is the concentration of free sodium caseinate ligand, and [AL] is the concentration of the complex of curcumin and sodium caseinate. The free concentrations of A and L are [A]=[A₀]-[AL] and [L]=[L₀]-[AL], respectively. [A₀] is the known concentration of the curcumin molecule and [L₀] is the known concentration of added sodium caseinate. Therefore, a quadratic fitting function for [AL] (www.nanotemper.com):

$$= 1/2 * (([A_0] + [L_0] + K_D) - \left(([A_0] + [L_0] + K_D)^2 - 4 * [A_0] * [L_0] \right)^{1/2}) \quad (8)$$

The signal obtained in the measurement directly corresponds to the fraction of curcumin molecules that formed the complex x = [AL]/[A₀], which can be easily fitted with the derived equation to obtain K_D.

Antioxidant activity

The 2,2'-azino-bis(3-ethylbenzothiazoline-6-sulphonic acid) (ABTS) antioxidant activities of native and NCP were determined according to the method reported in the literature with a slight modification (Nagaraju et al. 2021). ABTS was dissolved at 7 mM in deionized water. Potassium persulfate was dissolved in the ABTS solution with a concentration of 2.45 mM and was allowed to stand in the dark at room temperature (21 °C) for 12–16 h before use. The ABTS solution was diluted with 10 mM phosphate-buffered saline (PBS) at pH 7 to an absorbance value of 0.70 at 734 nm and equilibrated at room temperature. 10 mg of native curcumin or NCP were dissolved in 10 ml of acetone. The amount of curcumin varied in NCP based on the composition. The 100 μl solution was diluted with 3 ml of 10 mM PBS buffer to achieve 20–40% of initial concentration and the absorbance reading was taken at 30 °C exactly 1 min after initial mixing for up to 6 min. Ten mM PBS was used as a blank in each run. Each sample was measured in duplicate, and the mean and standard deviations were calculated. The scavenging capability of test compounds was determined using the following equation:

$$\text{Scavenging activity \%} = \frac{A_{control} - A_{sample}}{A_{control}} \times 100 \quad (9)$$

where, A_{sample} and A_{control} are the equilibrium absorbance of the test sample and the control, respectively.

In-vitro release kinetics at gastro-intestinal pH

75 mg of native curcumin powder and nano-curcumin-powder were dissolved in 1.5 ml of PBS to study the *in-vitro* release profile. The pH of phosphate buffer solution (PBS) was adjusted to 2.0 with HCl to mimic gastric

conditions and at pH 7.4 (15 ml 0.01 M NaOH) for intestinal conditions. The solutions were divided into 5 Eppendorf (0.20 ml each) tubes and put in a shaker at 37 ± 0.5 °C at 200 rpm. At designated time intervals the tubes were taken out and centrifuged at 3000 rpm for 5 min. The curcumin released (0.20 ml) was collected in the form of a pellet and re-suspended in 1 ml of acetone. The solution was filtered with 0.45-micron syringe filter to determine the amount of curcumin released using UV–Vis spectroscopy. The experiments were performed in duplicates.

Antimicrobial studies

The organisms, *Staphylococcus aureus* (MTCC7443), *Bacillus cereus* (MTCC 1305), *Escherichia coli* (MTCC 118), *Bacillus subtilis* (MTCC 441), *Pseudomonas aeruginosa* (MTCC 2297), *Pseudomonas aeruginosa* (MTCC 741), *Chromobacterium violaceum* (MTCC 2656), were obtained from Microbial Type Culture Collection (MTCC), Institute of Microbial Technology (IMTECH) Chandigarh, India. The aforementioned organisms were cultured for 24 h at 37 °C in Nutrient broth (NB) and Luria broth (LB) media and maintained at 4 °C. The chemicals and petriplates were procured from Hi-Media Ltd., Mumbai, India.

Agar well diffusion method: The antibacterial activity was carried out using the agar well diffusion method. The bacterial strains (18–24 h old) were grown on nutrient broth and incubated at 37 °C. The culture broth of 0.1 ml containing 10^8 – 10^9 cells cfu/ml was spread on nutrient agar plates by the spread plate method. The bored wells (8 mm diameter) in the agar plates were filled with 200 μ L (400 μ g/ml) of the native curcumin and nanocurcumin samples. The same volume of the negative control (distilled water) and positive control, Penicillin G (10 units), was also introduced into a well of all the plates. The incubated plates were used for measuring the zone of inhibition for its antibacterial activity and were expressed in terms of average diameter (millimeter). An inhibition diameter of less than 5 mm was interpreted as having no antibacterial activity. The assay was repeated 3 times and the data were statistically analyzed.

Statistical analysis

Three parallel experiments were carried out for all the analysis. The results are represented in the mean \pm standard deviation. Data were subjected to one-way ANOVA using (SPSS 11.5 software) to determine significant differences when $P < 0.05$.

Results and discussions

Morphology and particle size

Figure 1 represents variation in average particle size (%) of the prepared curcumin nanoemulsion concerning lipid: curcumin ratio. Gradual increase in lipid: curcumin ratio from 1 to 2: 0.05 to 0.2 increased droplet or spray dried particle size from 30 nm to 2 μ m. The unimodal peak distribution of particles converted to bimodal peak distribution in emulsion where, the particles of lowest and highest size prominently dominated the peaks, as shown in Fig. 1. This was attributed to the flocculation of the smaller particles or their mutual overlapping. The smallest mean particle size (33 nm) was observed for the sample having lipid: curcumin 1.0: 0.05 while the largest particle size ($\sim 2\mu$) was observed for lipid: curcumin 2.0:0.2. The low polydispersity of the former indicates an optimized ratio of the lipid, core and carrier material that overlaps the oil phase leading to the formation of smaller droplets. As the volume of the oil phase increases, the amount of carrier material is insufficient to overlap the core leading to the flocculation of smaller droplets due to thermodynamic instability of the nanoemulsion (Velokov KP and Pelan E, 2008). The SEM (Fig. 2) images were used to study the morphology of treated sodium caseinate (absence of milk fat and curcumin while keeping other conditions the same), native curcumin, NCP with milk fat: curcumin 1.0: 0.05 and 2.0: 0.1 samples. The treated sodium caseinate (Fig. 2a) has a smooth surface with an irregular shape showing its amorphous nature while the crystalline nature of native curcumin is evident in SEM (Fig. 2b). The sample with milk fat: curcumin ratio 1.0: 0.05 (Fig. 2c) exhibited spherical particles, majorly, with a few distorted trigonal shaped particles. A clear boundary around all the particles indicates a proper coating of carrier on the core material. The TEM (Fig. 2d) further confirms the uniform spherical and small size of the particles. Milk fat: curcumin ratio of 2.0: 0.1 resulted in the formation of irregular-shaped big particles with many dents on the surface (Fig. 2e). This could be attributed to an excess of lipid and core material compared to the carrying amount that lead to leaching of oil phase on the surface. Similar dents were observed with butterfat and sodium caseinate emulsion preparation (Faldt and Bergenstahl 1995). A possible explanation is, that the presence of fat crystals makes the emulsion unstable and facilitates the coalescence while an excess amount leads to their leaching on the surface. Contrary to nanoemulsions, a unimodal particle size distribution curve of spray-dried

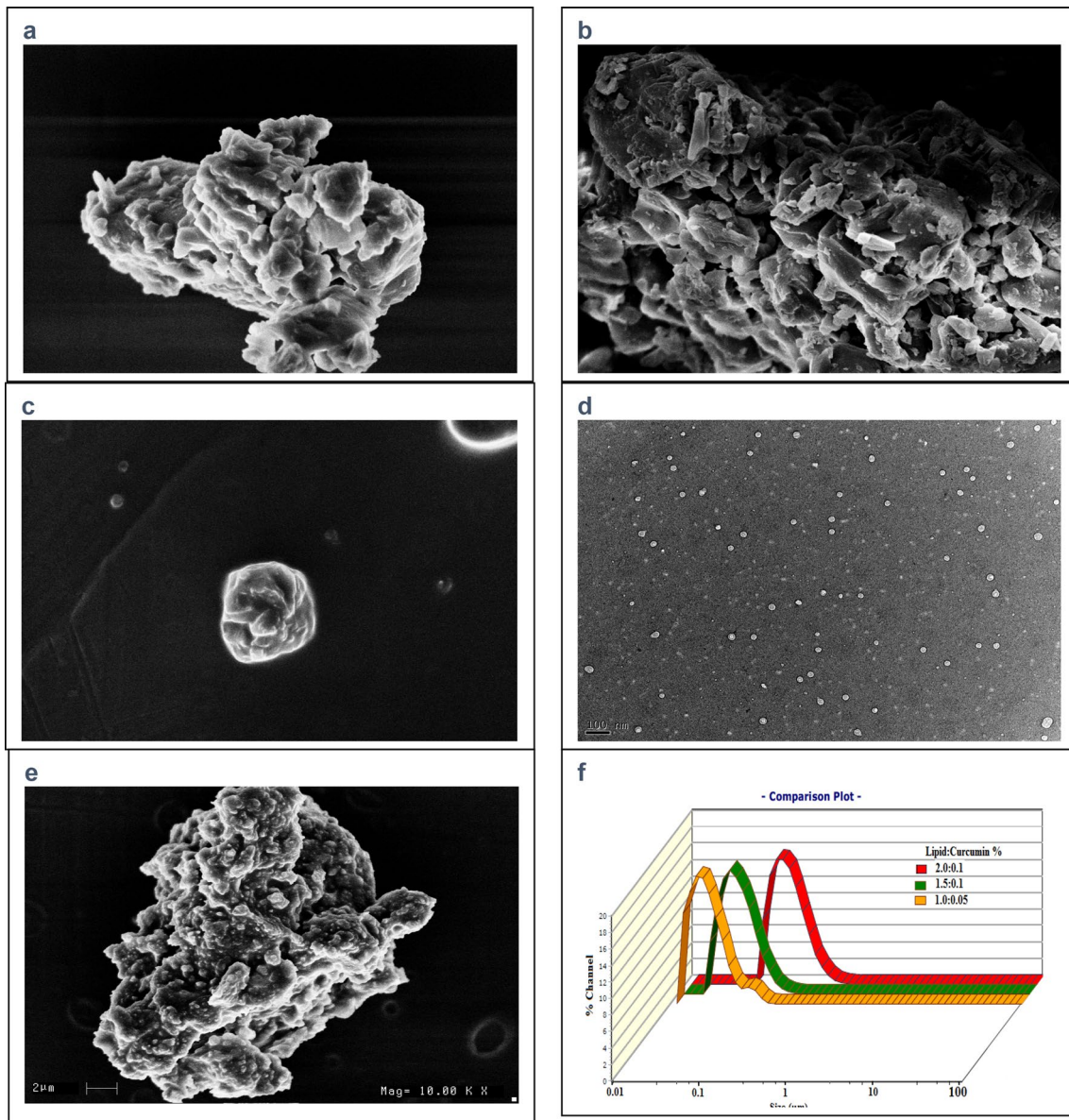


Fig. 2 SEM of **a** Treated sodium caseinate **b** Curcumin **c** NCP lipid: curcumin 1:0.05 **d** TEM NCP samples lipid: curcumin 1:0.05 **e** NCP lipid: curcumin 2:0.1 **f** Particle size distribution on lipid:curcumin ratio variation

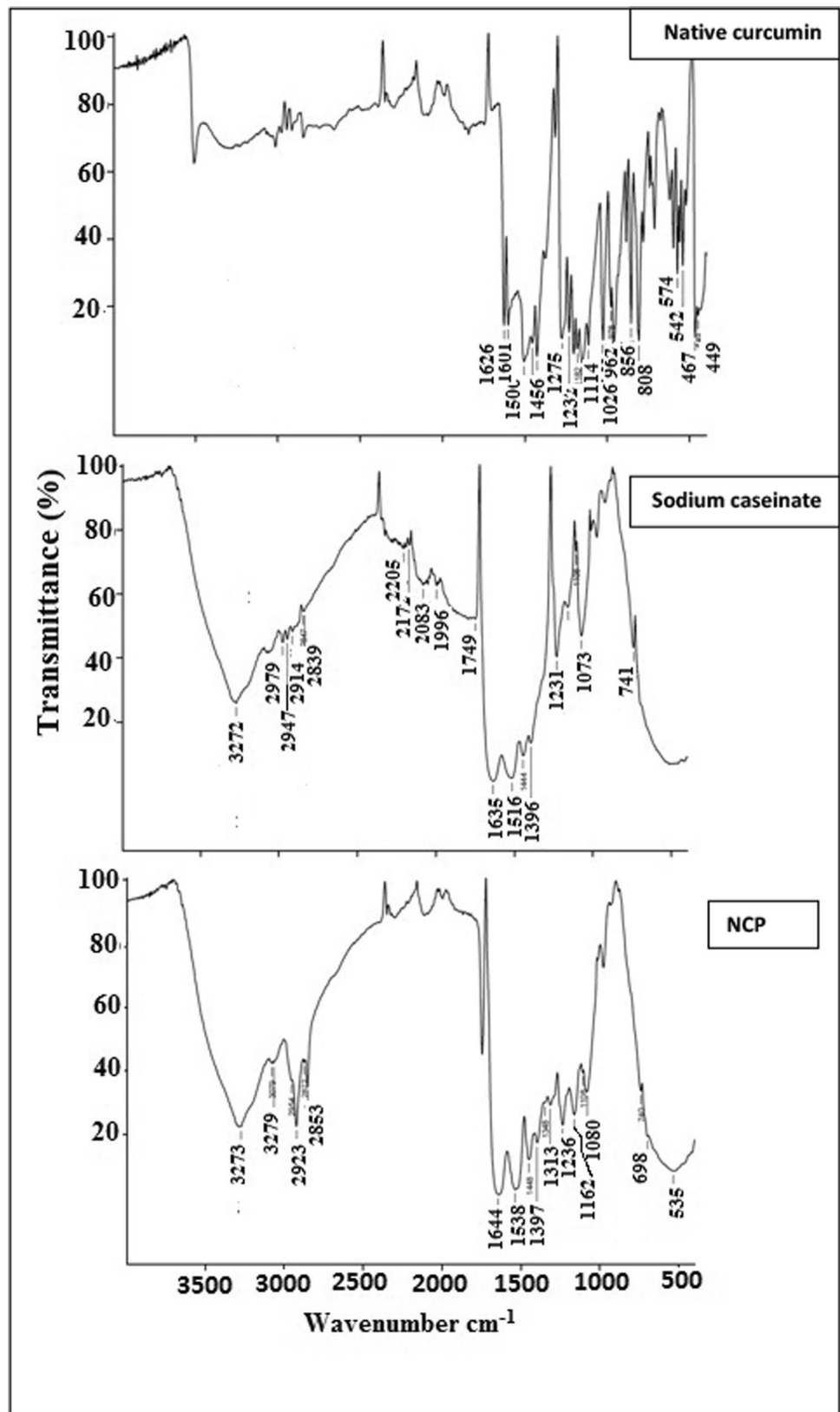
samples were obtained where; the average size was less than nanoemulsion droplets (Fig. 2f). The removal of moisture and disintegration of flocculated droplets under strong air-current of spray dryer resulted in uniform distribution of particles.

Structure elucidation

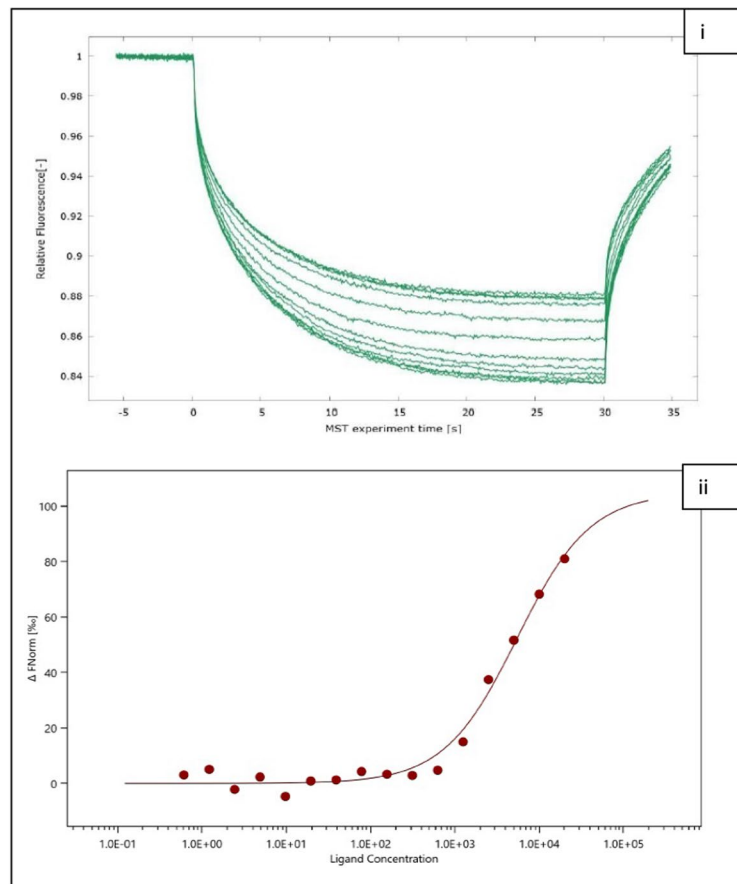
FTIR spectra (Fig. 3) were used to study the nature of bonding and interaction between curcumin and sodium caseinate after nanoencapsulation. Table 1 enlists the peaks attributed to functional groups and bonding vibrations belonging to curcumin, sodium caseinate, and NCP. In the curcumin

spectrum, all the significant peaks responsible for the hydroxyl groups, keto-enol form, aromatic methoxy groups, aromatic carbon-carbon stretching and carbon-hydrogen vibrations were clearly visible and closely match with the literature data (Kolev et al. 2005). The characteristic absorbance peak responsible for the stretching vibration of the -OH group in the curcumin molecule was observed at around 3500 cm^{-1} while it was not visible in the NCP indicating complete encapsulation or masking of the curcumin by the carrier. The peaks corresponding to the carbonyl group ($1800\text{--}1650\text{ cm}^{-1}$) were absent in spectra that indicated the presence of curcumin in the keto-enol tautomeric form (Mangolim et al. 2014). The peak at wavenumber 1275 cm^{-1}

Fig. 3 a FTIR spectra of native curcumin, sodium caseinate and NCP sample. **b** (i) Microscale thermophoresis curve exhibiting change in curcumin fluorescence w.r.t. sodium caseinate concentration from 20 μ M to 0.61 nM, (ii) Normalized MST relative fluorescence, F_{norm} Binding curve, after curcumin interaction with sodium caseinate



a FTIR spectra of native curcumin, sodium caseinate and NCP sample

Fig. 3 (continued)

b (i) Microscale thermophoresis curve exhibiting change in curcumin fluorescence w.r.t. sodium caseinate concentration from 20 μ M to 0.61 nM, (ii) Normalized MST relative fluorescence, F_{norm} Binding curve, after curcumin interaction with sodium caseinate

can be attributed to in-plane vibrations of CC-C and CC-H of the phenyl ring attached to the “keto” part, and H-C=O of the “keto” part of curcumin. The peaks observed at 1626, 1600, and 1506 cm^{-1} in native curcumin were not seen in NCP and were probably masked by a strong amide I band of protein, sodium caseinate. Similarly, the peaks related to the in-plane vibrations of CCC, CCH, and C-O-H of aromatic rings attached to the enolic part at 1427, 1185, and the CCH of a skeletal ring of curcumin at 1154 cm^{-1} were also not observed in NCP FTIR profile. Different peaks in the region of 1182 to 808 cm^{-1} corresponding to the vibrations of carbon-carbon, carbon-oxygen-carbon, carbon-hydrogen bonding in the aromatic ring, and being part of keto- or enol- form were also observed. The FTIR profile of sodium caseinate exhibited strong bands at 1635 and 1516 cm^{-1} , indicative of amide I and II bands, respectively. The amide I band mainly represents the C=O stretching vibrations of the amide groups coupled with the stretching of the C-N group and the amide II band is due to the in-plane bending of the N-H bonds (Surewicz WK, 1996). Another big and

broad band at 3272 cm^{-1} was due to the presence of free O-H and N-H groups of protein or sodium caseinate. The peak at 1076 cm^{-1} may be a contribution of different groups such as out-of-plane bending vibration of C-H (from aromatic structures) and PO^{2-} or P-OH bending vibration from phosphate ester, which is present in a significant amount in sodium caseinate in serine residues (Barreto et al. 2003). The peak at 1231 cm^{-1} is attributed to C-C(O)-C stretching vibrations of esters present in sodium caseinate. Other peaks in the lower energy region such as 1397–1440 cm^{-1} represent in-plane C-H bending and stretching vibration of C-C in aromatic structures. The C-H stretching vibrations of CH_2 and CH_3 were observed between 2900 to 2800 cm^{-1} region. The FTIR of NCP exhibited a shift in amide I and II band to a higher frequency (1644 cm^{-1} and 1538 cm^{-1}) that indicated protein structural changes due to the encapsulation process. Two new small peaks at 1313 and 1162 cm^{-1} were also seen in NCP, which may be attributed to the change in the conformational structure of casein sheets due to the establishment of interaction with either lipid solubilized curcumin or lipid during encapsulation. During emulsion

Table 1 Assignment of FTIR peaks of curcumin, sodium caseinate and NCP

Curcumin cm^{-1}	Sodium caseinate cm^{-1}	nano-cur-pdr cm^{-1}	Peak assignment
808			Out of plane bending of CC-H of phenyl ring attached to keto part of curcumin
851			Out of plane bending of C-H bond of phenyl CCH and skeletal CCH
1026			Out of plane bending vibrations of CH_3 and in-plane bending of CCH of aromatic ring positioned to the “enolic” part of curcumin
	1076		Out of plane bending vibration of C-H (aromatic), P-OH of phosphate residue
1114			Vibrational stretching of O- CH_3 and in-plane bending vibrations of CCH of aromatic rings
1154			In-plane bending of CCH in skeletal structure and phenyl ring attached to enolic part
1185, 1427			CCC, CCH and C-O-H of aromatic rings attached to the enolic part
1275			CC-C and CC-H of the phenyl ring attached to the keto part, and H-C=O of the keto part of curcumin
		1313, 1162	C-C stretch of aliphatic carbon linked to C=O of amide group
	1397	1397	C-N stretch of N of amino acids bonded with aromatic ring
1506			Stretching vibration of C=C and in-plane bending of CC=O
	1516		N-H bending of CONH group
1600, 1626			Stretching vibration of C=C and C=O
	1635		Stretching vibration of C=O of amide group (band I)
		1644, 1538	amide I and II band
	1516		In-plane bending of N-H of protein (band II)
	1440		Aromatic C-C stretching
	2900–2800		Stretching vibration of CH_2 and CH_3
	3272		Free O-H and N-H group of protein
3500			Stretching vibration of -OH group in curcumin

formation, the proteins are adsorbed at the oil/water interface where it unfolds to reorient, rearrange, and spread to form a continuous cohesive interface layer (Lee et al. 2007). The hydrophobic side chains orient towards the oil or lipid phase while hydrophilic polar groups bind with the aqueous phase where the O-H group of polyphenols forms intermolecular hydrogen bonding with free O-H and N-H group of sodium caseinate. The spray-drying locks the groups in the said position explaining the alteration in protein structure as confirmed by shifts in FTIR Amide bands.

Binding affinity

The MST is an ideal method for studying binding affinity because of its high sensitivity towards binding-induced changes in protein size, charge, or conformation. The dissociation constant, K_D , is inversely related to the binding affinity. The lower the dissociation constant higher is the affinity and vice versa. Figure 3b(i) shows curcumin fluorescence quenching under a thermal gradient with a change in protein concentration. The quenching of the fluorescence intensity is attributed to the binding of the ligand to the

fluorescent molecule. MST analysis is done by MO Affinity Analysis software and the K_D value obtained under specified conditions of this interaction is $4.7 \pm 0.05 \mu\text{M}$. Each MST curve is used to generate the normalized MST relative fluorescence, F_{norm} binding curve (Fig. 3b(ii)), of K_D of $4.7 \pm 0.05 \mu\text{M}$. The inverse of K_D resulted in a binding affinity of $2.1 \times 10^5 \text{ M}^{-1}$ between curcumin and sodium caseinate. The binding of curcumin with β -lactoglobulin milk protein was reported to be $2.4 \times 10^4 \text{ M}^{-1}$ and $1.1 \times 10^5 \text{ M}^{-1}$ at pH 6.5 and 7.0, respectively (Sneharani et al. 2010) due to hydrophobic interaction.

Lipid solubility, protein-fat %, and curcumin encapsulation efficiency

The figure (online resource1) shows the solubility weight % of curcumin in 1 ml of milk fat concerning varied curcumin concentrations. With the increase in curcumin concentration, the solubility % decreases from 21.9 to 2.4% due to the saturation concentration. Nonetheless, this value (2.4%) is at par with the value reported earlier for the solubility of curcumin in Tributyrin (2.94%), an SCT, and an expensive

Table 2 Influence of lipid:curcumin ratio on encapsulation efficiency and loading efficiency of nanoencapsulated curcumin

Lipid: Curcumin: Sodium caseinate ratio (w/w/w)	Encapsulation Efficiency %	Theoretical Loading %	Actual Loading %	Loading efficiency %
1.0:0.05:5.0	90.9±0.3	0.90	0.81±0.02	90.0
1.0:0.1:5.0	81.49±0.52	1.96	1.59±0.05	83.72
1.5:0.1:5.0	89.69±0.49	1.51	1.28±0.04	84.76
2.0:0.1:5.0	91.6±0.48	1.40	1.29±0.03	92.14

lipid. The solubilization % of bioactive (curcumin) in lipids is directly proportional to the high loading % in nanoparticles and consequently its high bioavailability. Thus, it is important to select an appropriate lipid, which ensures high solubility of curcumin and is reasonably priced from the food industry’s viewpoint. The process employed in the present study is cost-effective and facilitates the tailoring of particles size as low as 24 nm with encapsulated fat 13% (18% w/w of total mixture added initially) and curcumin loading efficiency of 90.0% and encapsulation efficiency of 90.73%. Milk fat is a mixture of SCT, MCT, and LCT where SCT makes 40% of the mixture helps in curcumin solubilization, and establishes a close dipole interaction with the curcumin while the percentage of MCT and LCT circumvent the oil diffusion through aqueous layer due to Ostwald ripening process (Kabalnov and Shchukin 1992). The effect of fat addition on the protein content of sodium caseinate has been shown in (online resource1). It is clear from the figure that the amount of protein/100 g of NCP sample decreases with an increase in fat content indicating the presence of lipid and core within the carrier sodium caseinate. However, no substantial change was observed in sodium caseinate nature due to the presence of lipids and encapsulation process (confirmed through SDS-PAGE, data not shown). Similar results were observed by (Sneharani et al. 2010). The encapsulation efficiency of representative samples with varied lipid:

curcumin ratio is given in Table 2. The highest encapsulation efficiency (~91%) obtained was for the sample having lipid: curcumin ratio 1:0.05, as curcumin is present in optimized concentration to be solubilized by the milk fat and finally, encapsulated by the sodium caseinate.

Anti-oxidant activity

The bioactivity of curcumin and NCP with different lipid-curcumin compositions was evaluated using ABTS scavenging free radical activity. ABTS is converted to radical cation after the addition of sodium persulfate and it gives absorbance at 734 nm. In the presence of polyphenolic antioxidant compounds, the ABTS gets reduced and converted back to the colorless neutral compound. The anti-oxidant activity of curcumin was compared before and after encapsulation. Table 2b indicates that the antioxidant activity of NCP with lipid: curcumin ratio 1:0.2 (w/w %) is equivalent to native curcumin. However, the 10 mg of NCP contains only 20 µg of curcumin as against the 10 mg of native curcumin dissolved in acetone. Thus, it can be said that the antioxidant activity of water-soluble NCP (with 20 µg of curcumin) is higher than native curcumin (10 mg). With an increase in lipid concentration in the NCP, the antioxidant activity decreased from 91 to 82% due to the low concentration of

Table 3 Influence of lipid:curcumin ratio on antioxidant activity of nanoencapsulated curcumin

Lipid: Curcumin: Sodium caseinate amount (w/w/w)	Curcumin concentration (µg/ml)	Antioxidant activity %
1.0:0.05:5.0	8.2/10 mg of sample	91.15±0.11
1.0:0.1:5.0	16.3/10 mg of sample	91.50±0.15
1.5:0.1:5.0	15.1/10 mg of sample	88.99±0.18
2.0:0.1:5.0	14.2/10 mg of sample	73.21±0.23
1.0:0.2:5.0	32.2/10 mg of sample	92.34±0.20
1.5:0.2:5.0	29.8/10 mg of sample	90.43±0.22
2.0:0.2:5.0	27.7/10 mg of sample	82.78±0.21
Native Curcumin	1000	96.16±0.6

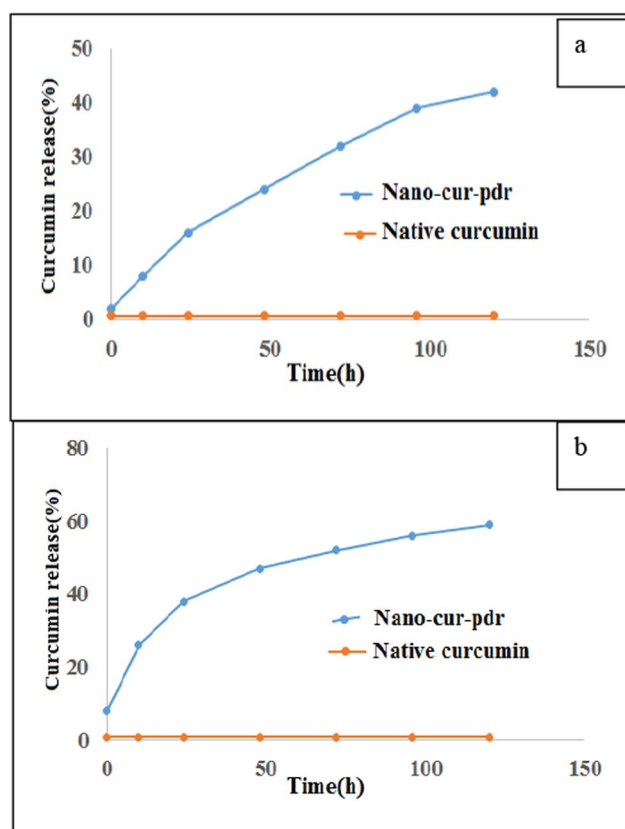


Fig. 4 *In-vitro* release profile of curcumin from NCP and native curcumin in phosphate buffer solution for 5 days **a** pH=2.0, **b** pH=7.4

curcumin molecule (Table 3) to reduce the ABTS cation. The increase in lipid concentration results in overlapping/agglomeration of particles leading to a less and very slow release of curcumin molecule compared to a sample with a small size (33 nm).

Lipolysis and *in-vitro* release

Using equations (online resource Eqs. 1 and 2), the extent of lipolysis of milk fat was calculated to be $54 \pm 3.6\%$ for the fed state and $62 \pm 4.2\%$ for the fasted state. Whereas, the % bioaccessibility (online resource Eq. 3) of curcumin

was calculated to be 44% and 52% for fasted and fed state, respectively. The UV–VIS spectroscopy based ASTA method was used to analyse curcumin content released from native and nanoencapsulated curcumin (lipid: curcumin ratio- 1:0.05) during *in-vitro* release at both 2.0 and 7.4 pH conditions (Fig. 4). A very fast release from NCP in the initial hours resulted in high curcumin content in the buffer solution. This is mainly due to the release of both unencapsulated or adsorbed curcumin from the sample and encapsulated curcumin. The release rate was quite slow and constant both in artificial gastric juice (pH 2.0; Fig. 4a) and in intestinal juice (pH 7.4; Fig. 4b) on the 4th and 5th days. The release process can be described as a two-step biphasic process where an initial burst is followed by a slow release. The cumulative released % of nano-curcumin was 60% at pH 7.4 and 40% at pH 2.0 while, cumulative % of native curcumin was 0.8% at pH 7.4 and 0.6% at pH 2.0. Higher solubility of nanoencapsulated curcumin in intestinal pH than gastric pH explains its enhanced bioavailability after nanoencapsulation and low solubility of native curcumin is attributed to its lipophilic nature. Since the absorption of food takes place in the intestine thus, the slow and controlled release of nanoencapsulated curcumin may be used to treat ailments by the pharma and food industry.

Antibacterial studies

Table 4 lists the zone of inhibition of selected strains of food-borne pathogens due to the activity of curcumin and nanoencapsulated curcumin. The inhibitory activity of nanoencapsulated curcumin was more pronounced against Gram-positive bacteria than Gram-negative bacteria. All the tested pathogens have experienced strong activity with nano-curcumin compared to native curcumin and it could be due to the small particle size and high solubility of the NCP. The curcumin nanoparticles manifest antibacterial properties by anchoring and breaking into the cell wall of the bacterial cell and then penetrating inside the cell leading to disruption of the structure of cell organelles (Gul and Bakht 2015).

Table 4 Antibacterial activities of native curcumin and nanocurcumin

Compound	Antibacterial activities (Zone of Inhibition (mm))					
	<i>B.subtilis</i>	<i>B.cereus</i>	<i>S.aureus</i>	<i>P.aeruginosa</i>	<i>E.coli</i>	<i>C.violaceum</i>
Curcumin (8 µg/ml)	16 ± 0.5	9 ± 0.5	15 ± 0.4	10 ± 0.2	9 ± 0.5	19 ± 0.5
Nano curcumin (6.4 µg/ml)	22 ± 0.5	18 ± 0.7	20 ± 0.5	20 ± 0.6	11 ± 0.4	21.0 ± 0.5
Penicillin G (Control)	28 ± 0.5	21.4 ± 0.2	10.5 ± 0.5	27.0 ± 0.2	29.2 ± 0.2	25 ± 0.5

Conclusion

The biological properties of nano-sized curcumin were extremely dependent on the lipid: curcumin ratio used in o/w nanoemulsion. The high solubility of curcumin in milk fat and digestion during lipolysis can increase its bioavailability. An optimized ratio of lipid: to curcumin is important to achieve encapsulated curcumin in size < 50 nm that controls the release of bioactive compound in a two-step biphasic way. The particles with smaller size (< 50 nm) showed enhanced anti-oxidant, and anti-microbial activity compared to native curcumin.

Acknowledgements The authors are grateful to Director, CSIR-CFTRI, Mysuru, for his permission to accomplish and publish this work. The authors are also thankful to the Head & staff, PPS&FT, CSIR-CFTRI, Mysuru, and CIFS facility at CFTRI, Mysuru for their support. The financial assistance for the research work from the Science & Engineering Research Board (SERB-DST), the Government of India, New Delhi (EMR/2016/005112) is appreciated. PJR is thankful to Saji, Nanotemper Technologies for performing MST studies.

Author's contribution PJR- C`onceptualization, methodology, writing- reviewing, editing and revision, HK- Analysis, PSM- Microbiological studies, data curation, SSV, MSN- Experimentation work.

Funding Science & Engineering Research Board (SERB-DST), Government of India, New Delhi (EMR/2016/005112).

Data availability The datasets used and/or analysed during the current study are available from the corresponding author on reasonable request.

Declarations

Conflict of interest Authors declare no competing interest.

Ethical approval The research work of this manuscript does not involve animal related studies. Therefore, approval of animal ethics committee is not required. Moreover, the authors have complied with ‘‘work ethics’’ during the manuscript preparation and submission.

Consent to participate PJR consents to participate in case of request.

Consent for publication The manuscript submission to Journal of Food Science and Technology (JFST) publication has been approved by all authors.

References

Ahmed K, Li Y, McClements DJ, Xiao H (2012) Nanoemulsion- and emulsion-based delivery systems for curcumin: encapsulation and release properties. *Food Chem* 132:799–807

Barreto PLM, Pires ATN, Soldi V (2003) Thermal degradation of edible films based on milk proteins and gelatin in inert atmosphere. *Polym Degrad Stab* 79:147–152

Bhawana D, Kumar Basniwal R, Singh Buttar H, Jain VK, Jain N (2011) Curcumin nanoparticles: preparation, characterization, and antimicrobial study. *J Agric Food Chem* 59:2056–2061

Bucurescu A, Blaga AC, Estevinho BN, Rocha F (2018) Microencapsulation of curcumin by a spray-drying technique using gum arabic as encapsulating agent and release studies. *Food Bioprocess Technol* 11:1795

Deck LM, Hunsaker LA, Vander Jagt TA, Whalen LJ, Royer RE, Vander Jagt DL (2018) Activation of anti-oxidant Nrf2 signaling by enone analogues of curcumin. *Eur J Med Chem* 143:854–865

Fuchs M, Turchiuli C, Bohin M, Cuvelier ME, Ordonnaud C, Peyrat-Maillard MN, Dumoulin E (2006) Encapsulation of oil in powder using spray drying and fluidised bed agglomeration. *J Food Eng* 75:27–35

Gul P, Bakht J (2015) Antimicrobial activity of turmeric extract and its potential use in food industry. *J Food Sci Technol* 52:2272–2279

Jiang T, Charcosset C (2022) Encapsulation of curcumin within oil-in-water emulsions prepared by premix membrane emulsification: Impact of droplet size and carrier oil type on physicochemical stability and in vitro bioaccessibility. *Food Chem* 375:131825

Kabalnov AS, Shchukin ED (1992) Ostwald ripening theory: applications to fluorocarbon emulsion stability. *Adv Colloid Interface Sci* 38:69–97

Kolev TM, Velcheva EA, Stamboliyska BA, Spiteller M (2005) DFT and experimental studies of the structure and vibrational spectra of curcumin. *Int J Quantum Chem* 102:1069

Kumar DD, Mann B, Pothuraju R, Sharma R, Bajaj R, Minaxi, (2016) Formulation and characterization of nanoencapsulated curcumin using sodium caseinate and its incorporation in ice cream. *Food Funct* 7:417–424

Lee SH, Lefèvre T, Subirade M, Paquin P (2007) Changes and roles of secondary structures of whey protein for the formation of protein membrane at soy oil/water interface under high-pressure homogenization. *J Agric Food Chem* 55:10924–10931

Mangolim CS, Moriwaki C, Nogueira AC, Sato F, Baesso ML, Neto AM, Matioli G (2014) Curcumin- β -cyclodextrin inclusion complex: Stability, solubility, characterisation by FT-IR, FT-Raman, X-ray diffraction and photoacoustic spectroscopy, and food application. *Food Chem* 153:361–370

Method 18, 4th ed (1997), Official analytical methods of the American Spice Trade Association (ASTA). New Jersey-07632, Englewood Cliffs.

Nagaraju PG, Sindhu P, Dubey T, Chinnathambi S, Poornima Priyadarshini CG, Rao PJ (2021) Influence of sodium caseinate, maltodextrin, pectin and their Maillard conjugate on the stability, in vitro release, anti-oxidant property and cell viability of eugenol-olive oil nanoemulsions. *Int J Biol Macromol* 183:158–170

Faldt P, Bergenstahl B (1995) Fat encapsulation in spray-dried food powders. *J Am Oil Chem Soc* 72:171–176

Pandey S, Vindya HA, Kumar A, Rao PJ (2022) Curcumin loaded core-shell biopolymers colloid and its incorporation in Indian Basmati rice: an enhanced stability, anti-oxidant activity and sensory attributes of fortified rice. *Food Chem* 387:132860

Paula VS, Ana CP, Lívia ND, Ana Paula Dias Ribeiro MCA and EG de OM (2018) Curcumin-mediated anti-microbial photodynamic therapy against *Candida dubliniensis* biofilms. *Lasers Med Sci* 33:709–717

Peng S, Zhou L, Cai Q, Zou L, Liu C, Liu W, McClements DJ (2020) Utilization of biopolymers to stabilize curcumin nanoparticles prepared by the pH-shift method: caseinate, whey protein, soy protein and gum Arabic. *Food Hydrocoll* 107:105963

Rao PJ, Khanum H (2016) A green chemistry approach for nanoencapsulation of bioactive compound - Curcumin. *LWT - Food Sci Technol* 65:695–702

Shankar Patel S, Pushpadass HA, Eljeeva Emerald Franklin M, Nath Battula S, Vellingiri P (2022) Microencapsulation of curcumin by

- spray drying: Characterization and fortification of milk. *J Food Sci Technol* 59:48
- Sheikhzadeh S, Alizadeh M, Rezazad M, Hamishehkar H (2016) Application of response surface methodology and spectroscopic approach for investigating of curcumin nanoencapsulation using natural biopolymers and nonionic surfactant. *J Food Sci Tech* 53:3904–3915
- Sneharani AH, Karakkat JV, Singh SA, Rao AGA (2010) Interaction of curcumin with β -lactoglobulin; stability, spectroscopic analysis, and molecular modeling of the complex. *J Agric Food Chem* 58:11130–11139
- Sun J, Zhao Y, Hu J (2013) Curcumin inhibits imiquimod-induced psoriasis-like inflammation by inhibiting IL-1 β and IL-6 production in mice. *PLoS One* 8:e67078
- Surassmo S, Min SG, Bejrapha P, Choi MJ (2010) Effects of surfactants on the physical properties of capsicum oleoresin-loaded nanocapsules formulated through the emulsion–diffusion method. *Food Res Int* 43:8–17
- MaH SWK (1996) Infrared absorption methods for examining protein structure. In: Havel HA (ed) *Spectroscopic methods for determining protein structure in solution*. VCH Publisher Inc
- Vegarud GE, Langsrud T, Svenning C (2000) Mineral-binding milk proteins and peptides; occurrence, biochemical and technological characteristics. *Brit J Nutr* 84:S91-98
- Velokov KP, Pelan E (2008) Colloidal delivery systems for micronutrients and nutraceuticals. *Soft Matter* 4:1964–1980
- Walstra P, Walstra P, Wouters JTM, Geurts TJ (2005) *Dairy science and technology*. CRC Press
- Publisher's Note** Springer Nature remains neutral with regard to jurisdictional claims in published maps and institutional affiliations.
- Springer Nature or its licensor (e.g. a society or other partner) holds exclusive rights to this article under a publishing agreement with the author(s) or other rightsholder(s); author self-archiving of the accepted manuscript version of this article is solely governed by the terms of such publishing agreement and applicable law.